

Distribution function of the local density of states of a one-channel weakly disordered ring in an external magnetic field

H. Feldmann, E. P. Nakhmedov,* and R. Oppermann

Institut für Theoretische Physik, Universität Würzburg, 97074 Würzburg, Federal Republic of Germany

(Received 21 January 2000)

A real space diagrammatic method, which is an extension of the Berezinskii technique to problems with periodic boundary condition, is formulated to study the density of states (DOS) $\rho(\epsilon, \phi)$ and its moments for a one-channel weakly disordered ring threaded by an external magnetic flux ϕ . The exact result obtained for the average value of the DOS shows that $\rho(\epsilon, \phi)$ oscillates with a period of the flux quantum $\phi_0 = hc/e$. However, all higher moments of the DOS oscillate with the halved period $\phi_0/2$. The exact expression for the DOS is valid for both weak localization ($L \gg l$, where L is the ring's circumference and l is the mean free path) and ballistic ($L \leq l$) regimes. In the weak localization regime the distribution function of the DOS is calculated, which turns out to be of logarithmic normal form.

I. INTRODUCTION

Interference effects in low-dimensional disordered conductors still attract attention from both experimental and theoretical physicists, although all main features and a lot of new effects have already been discovered during the last 20 years. The prediction of the oscillation in the kinetic coefficients in multiply connected disordered normal metals in an external magnetic field¹ and its experimental observation² in a Mg cylinder was a very excellent examination of weak localization phenomena, since the coherence of the electron wave function during the circulation of a closed contour is required to observe an oscillation. The period of oscillation of the magnetoresistance predicted and observed first was equal to half of the magnetic flux quantum $\phi_0 = hc/e$. Further improvements of the experiments on rings with large diameters and small widths gave rise to the observation of a magnetoresistance oscillation with the period ϕ_0 (Ref. 3); furthermore in the experiment of Chandrasekhar *et al.*⁴ both periods were observed.^{5,6} Such a complex magnetic field dependence of the magnetoresistance seems to be related to the statistical properties of the sample.

Another development in theory was the prediction of a persistent current in a one-channel disordered isolated loop.⁷ Due to the analogy between the loop and one-dimensional (1D) lattice with a period equal to the circumference of the loop, a circulating current in rings was suggested, which is a periodic function of the enclosed flux with a period of ϕ_0 . Studies of the effects on the persistent current at finite but small temperature and weak inelastic scattering show that both weak inelastic and elastic scattering do not destroy it.⁸⁻¹¹ In experiments, the persistent current was also observed.¹²⁻¹⁵ A magnetization measurement was performed in Ref. 12 on $N = 10^7$ disconnected copper loops at $T < 1.5$ K where the electron phase coherence length L_ϕ exceeds the loop's circumference $L = 2.2 \mu\text{m}$, and it shows evidence for a flux-periodic persistent current with halved period and $3 \times 10^{-3} e v_F / L$ amplitude per ring, which is remarkably higher than the theoretically expected value for the persistent current per ring, $\sqrt{(l/LN)}(e v_F / L)$.^{10,16,17} Measurements of

the persistent current on single loops (with at least a few channels) in the diffusive¹³ ($L = 8 \mu\text{m}$ and $l = 70$ nm, where l is the elastic mean free path) and ballistic¹⁴ ($L = 8.5 \mu\text{m}$ and $l = 11 \mu\text{m}$) regimes reveal the period ϕ_0 . The amplitude of the harmonic with $\phi_0/2$ was measured to be smaller by a factor of 2-3 than that of the ϕ_0 harmonic in Ref. 13.

Effects of impurities in most of the theoretical investigations were taken into account by the transfer matrix method according to the Landauer expression and by generalizations of this method to n -channel systems.^{18-20,11} Although the Landauer formula gives full-flux periodicity for all physical parameters, averaging over ensembles of rings^{9,16,17,21-24} or the calculation of the dynamical current instead of the thermodynamical potential²⁵⁻²⁸ was suggested as an explanation of the observed halved periodicity. In the process of averaging over different impurity realizations in the ensemble, the number of particles in each ring is proposed to be constant, i.e., the persistent current is assumed to be determined by the thermodynamic potential instead of the grand canonical potential.²²⁻²⁴ Although there has been much work done on the Aharonov-Bohm effect, the existing theories of non-interacting electrons still can explain neither the high value of the experimentally observed persistent currents¹²⁻¹⁵ nor its diamagnetic sign.¹⁵ This can be partially connected with the complexity of the experiments, particularly with difficulties of the separation of phase effects in the rings with relatively large width (larger than the mean free path^{12,15}) from orbital ones.

On the other hand, correlation effects may be a reason for the discrepancy between theory and experiment.²⁹⁻³⁸ Unfortunately, there is still no agreement on the effects of Coulomb interaction on the amplitude of the persistent current. Studies based on spinless electrons in the 1D continuum^{29,31,32} and lattice models³³⁻³⁵ gave controversial results, so the amplitude of the persistent current was shown to be increased up to its disorder-free value according to the former model, but a Mott-Hubbard metal-insulator transition in the latter model was found to reduce the amplitude, or at least a possible increase of the amplitude was negligibly small. There was also the suggestion that correlation can

change the fundamental period with the magnetic flux and create fractional periodicity in a 1D ring.³⁸ Impurities and correlation acting together are again subject of controversy. Thus, considering weak localization corrections in first order in the electron-electron interaction to the grand canonical potential,³⁰ a persistent current with a period of $\phi_0/2$ and an amplitude of $\sim ev_F l/L^2$, corresponding to the experiment,¹² was obtained, while Monte Carlo simulation on a 1D Luttinger liquid³⁹ resulted in a persistent current with period ϕ_0 and with an amplitude decreased through interaction. Resumming the existing results it can be said that neither the noninteracting electron model nor models of correlated electrons yet gave satisfactory answers to the questions put forward by the experiments. These concern the period (under what condition both periods or only the halved period are observed), the amplitude of the persistent current, and its diamagnetic sign (for the correlated electron model the diamagnetic sign requires an attractive interaction between the electrons).

To prevent the interference of the orbital effects in the presence of an external magnetic field with the phase effects,

the width of the ring should be chosen as narrow as possible, i.e., a one-channel ring with random impurities seems to be an ideal tool to study the Aharonov-Bohm effect. However, interference effects in 1D disordered systems as a result of the coherent backscattering processes are strong⁴⁰ irrespective of the degree of randomness. The diffusion approximation, which was used in previous studies, is not acceptable in 1D systems even for the case of weak disorder.

Approaching the problem thoroughly, we use in this paper a weakly disordered noninteracting electron model and construct for it a new exactly solvable diagrammatic method, which is an extension of Berezinskii's method^{41,42} to the problem with periodic boundary conditions. Within this model, we sum all impurity scattering diagrams in the framework of the Born approximation.

In Sec. II, we describe the method. We calculate the density of electronic states (DOS) in Sec. III. Indeed an average value is not enough to describe the observable parameters in low-dimensional mesoscopic systems. It is well known that the physical parameters of a mesoscopic system with size L satisfying the condition $l < L \ll L_\phi$ fluctuate from sample to sample, i.e., self-averaging is violated.⁴³⁻⁴⁵ At $T=0$ all sufficiently large systems become mesoscopic. In this case, high moments give a considerable contribution,⁴⁶⁻⁵² which results in strong differences between average value and typical one of the observable parameter, i.e., the average value loses its significance to characterize the experimental observation. In Sec. IV the diagrammatic method is applied to find the k th moments of the DOS, $\langle \rho^k(\epsilon, \phi) \rangle$. The obtained equations for $\langle \rho^k(\epsilon, \phi) \rangle$ show that, in contrast to the average value of the DOS, all higher moments oscillate with the halved period, $\phi_0/2$. Although the structure of the equations is complicated, the latter can be solved for the weak localization regime when the condition $l \ll L$ is satisfied. This procedure is given in Sec. V.

The zeroth (not depending on ϕ) and the first (oscillating with $\phi_0/2$) harmonic of $\langle \rho^k(\epsilon, \phi) \rangle$ are studied explicitly in this section. Both are shown to increase with k as $\exp(k^2)$, which gives rise to a logarithmic normal distribution. In Sec. VI we conclude our results and discuss possibilities to extend our approach to related problems.

II. DESCRIPTION OF THE METHOD

We consider here a one-channel disordered ring with length $L=2\pi r$, threaded by a magnetic flux ϕ through the opening. The Hamiltonian of the system can be written as

$$H = \frac{\hbar^2}{2m^*r^2} \left(i \frac{\partial}{\partial \varphi} + \frac{\phi}{\phi_0} \right)^2 + V_{\text{imp}}(\varphi), \quad (1)$$

where $\phi_0 = hc/e$ is the fundamental period of a flux quantum and m^* is the effective mass of an electron. The potential V_{imp} of randomly distributed impurities is considered to be weak, so that scattering processes can be studied in the framework of the Born approximation. Below, we use the spatial variable $x=r\varphi$ instead of the angle φ .

Our aim in this section is to construct a diagrammatical method for the calculation of the average values of the DOS, $\langle \rho(\epsilon, \phi; L) \rangle$, and of its moments $\langle \rho^n(\epsilon, \phi; L) \rangle$. The bracket $\langle \dots \rangle$ denotes the average over the impurity configurations. Expressing the DOS by means of retarded (G_R) and advanced (G_A) Green's functions (GF) as

$$\begin{aligned} \rho(\epsilon, \phi; x) &= -\frac{1}{\pi} \text{Im} G_R(\epsilon, \phi; x, x) \\ &= \frac{1}{2\pi i} [G_A(\epsilon, \phi; x, x) - G_R(\epsilon, \phi; x, x)], \end{aligned} \quad (2)$$

the k th moment of $\rho(\epsilon, \phi; x)$ can be given by

$$\begin{aligned} \langle \rho^k(\epsilon, \phi; x) \rangle &= \frac{1}{(2\pi i)^k} \sum_{l=0}^k \binom{k}{l} (-1)^l \\ &\quad \times \langle G_R^l(\epsilon, \phi; x, x) G_A^{k-l}(\epsilon, \phi; x, x) \rangle. \end{aligned} \quad (3)$$

The Berezinskii diagram technique^{41,42} is applied to calculate the average value of a single GF and higher-order correlators $\langle G_R^l G_A^{k-l} \rangle$. In contrast to strictly 1D disordered wires, quantum corrections to the DOS of a ring turn out to exist even for the weakly disordered limit due to periodicity.

As for infinite systems, we consider as starting point a free particle with wave function $\psi_p(x) \propto \exp(ipx)$, where the momentum can assume arbitrary values, leading to a continuous spectrum $\epsilon_p = (\hbar^2/2m^*)(p - \phi/\phi_0 r)^2$. The "bare" GF $G_{R,A}^0$ can be calculated easily:

$$\begin{aligned} G_{R,A}^0(\epsilon, \phi; x, x') &= \int \frac{dp}{2\pi} \frac{e^{ip(x-x')}}{\epsilon - \epsilon_p \pm i\eta} \\ &= \mp \frac{i}{v(\epsilon)\hbar} \\ &\quad \times e^{i2\pi(\phi/\phi_0)(x-x')/L \pm i\pi(\epsilon)|x-x'| - [i\eta/v(\epsilon)]|x-x'|}, \end{aligned} \quad (4)$$

where L is the circumference of the ring and the parameter η is introduced phenomenologically to model inelastic processes, which result in a blurring of the energy levels. $v(\epsilon)$

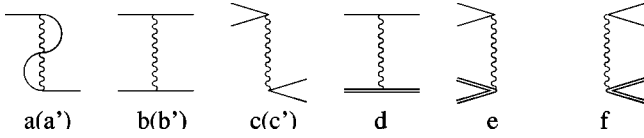


FIG. 1. Contributing internal vertices. Vertices a' , b' , and c' have the same form as a , b , and c , but double lines instead of single ones. The following factors correspond to the vertices: a,a' : $\sim(-1/2l^- - 1/2l^+)$; b,b' : $\sim-1/l^+$; c,c' : $\sim-1/l^-$; d : $\sim(+1/l^+)$; e : $\sim(+1/l^-)\exp[4\eta x/v(\epsilon)]$; f : $\sim(+1/l^-)\exp[-4\eta x/v(\epsilon)]$.

$=\sqrt{2\epsilon/m^*}$ and $\hbar p(\epsilon) = \sqrt{2m^*\epsilon}$ are the velocity and the momentum of an electron with energy ϵ , respectively. Notice that Zeeman splitting has not been taken into account here. For an electron with spin $s = \pm \frac{1}{2}$, it would throughout the paper lead to a shift of the energy as $\epsilon \rightarrow \epsilon - sg\mu_B B$ (where g is the gyromagnetic ratio of the electron and μ_B is the Bohr magneton).

This bare GF, however, is not yet the real GF for an electron in a ring without impurities, since it does not reflect the finite size of the system and the periodic boundary conditions. These are taken into account by allowing the particles to make arbitrary revolutions around the ring, which leads to the expected quantization effect. According to this prescription, the GF for a clean ring $\tilde{G}_{R,A}^0$ is

$$\begin{aligned} \tilde{G}_{R,A}^0(\epsilon, \phi; x, x') &= G_{R,A}^0(\epsilon, \phi; x, x') + G_{R,A}^0(\epsilon, \phi; x, x' + L) \\ &+ G_{R,A}^0(\epsilon, \phi; x, x' - L) \\ &+ G_{R,A}^0(\epsilon, \phi; x, x' + 2L) + \dots \end{aligned} \quad (5)$$

One may verify this approach by calculating the DOS of a clean ring in a magnetic field $\rho_0(\epsilon, \phi)$ from Eqs. (2), (4), and (5):

$$\begin{aligned} \rho_0(\epsilon, \phi) &= \rho_0 + 2\rho_0 \sum_{n=1}^{\infty} \cos[p(\epsilon)Ln] \cos\left(2\pi \frac{\phi}{\phi_0} n\right) \\ &\times e^{-[\eta/v(\epsilon)]Ln}, \end{aligned} \quad (6)$$

where $\rho_0 = 1/[\pi\hbar v(\epsilon)]$ is the DOS for a pure and infinite 1D system. As $\eta \rightarrow 0$, Eq. (6) displays the discrete behavior for the DOS of a clean ring.

In the diagrammatical technique, the retarded (advanced) GF of an electron moving in the field of randomly distributed impurities is represented by an ordinary (double) continuous line in real space, which goes from point x to x' after multiple scattering on a given impurity configuration, realized by the potentials $V(x_i)$ with impurities placed at the points $\{x_i\}$.

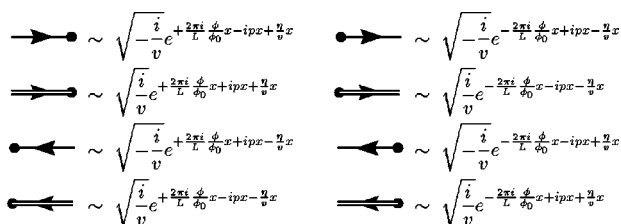


FIG. 2. The external vertices. One incoming vertex and one outgoing vertex are attached to each continuous fermion line characterizing one Green's function.

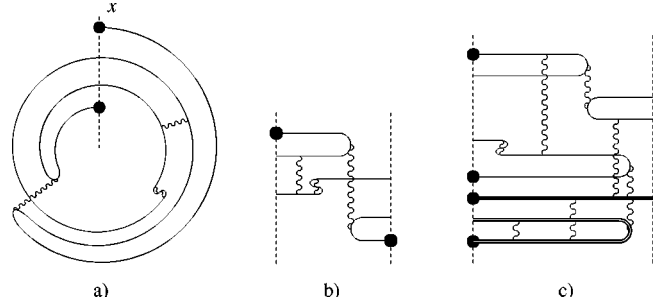


FIG. 3. A simple diagram contributing to the single GF $\langle G_R \rangle$ (a) resembling the motion of the electron around the ring and (b) after cutting at point x . The numbers characterizing this diagram are $m = 1$ and $n = 1$. (c) shows a contribution to $\langle G_R G_A \rangle$. Here, $m = 2$, $m' = 1$, $n = 0$, $\bar{m} = 1$, $\bar{m}' = 0$, and $\bar{n} = 1$.

For the DOS and its moments it suffices to consider $x = x'$. Since the ‘‘bare’’ GF’s [Eq. (4)] between two successive scatterings have factorable structure, the coordinate dependence can be transferred from the lines to the vertices. Averaging over the random Gaussian potential leads to a pairing of the impurity vertices. Their strength is measured by the inverse forward (backward) scattering length,

$$\begin{aligned} \frac{1}{l^+(\epsilon)} &= \frac{2}{\hbar^2 v^2(\epsilon)} \int_0^{\infty} U(x) dx, \\ \frac{1}{l^-(\epsilon)} &= \frac{2}{\hbar^2 v^2(\epsilon)} \int_0^{\infty} U(x) dx \cos[p(\epsilon)x]. \end{aligned} \quad (7)$$

For the Born approximation to be applicable, the correlator $U(x-x') = \langle V(x)V(x') \rangle$ should have a width much smaller than the mean distance between impurities $1/c$, and $1/c \ll l^{\pm}$. In the extreme case of a white noise potential $U(x-x') = cU_0^2 \sum_{n=-\infty}^{\infty} \delta(x-x'+nL)$, the two scattering lengths become equal, $l^- = l^+ = 2l$. Given in Fig. 1 are the essential vertices selected according to the condition $p_F l \gg 1$, with p_F and l being the Fermi momentum and the mean free path, respectively. Although the ‘‘bare’’ GF’s depend on the direction due to the magnetic field, the internal vertices in Fig. 1 do not differ from those of Berezinskii. All dependence on the magnetic field is transferred from the lines to the external vertices, which are shown in Fig. 2.

As an example, a simple diagram contributing to $\langle G_R(\epsilon, \phi; x, x) \rangle$ is drawn in Fig. 3(a). For convenience, we cut the diagram at point x and straighten the lines, which results in Fig. 3(b). Each diagram for a single GF is then characterized by m pairs of lines returning to x and n through-going lines. Since the bulk of each diagram (i.e., after the removal of the external vertices) does not depend on the direction, n is the sum of right-going n^+ and left-going n^- lines. For correlators $\langle G_R^l(\epsilon, \phi; x, x) G_A^{k-l}(\epsilon, \phi; x, x) \rangle$, we have to distinguish the number m of returning lines on the left-hand side (lhs) and the number m' of returning lines on the rhs, and in addition we must introduce \bar{m} , \bar{m}' , and \bar{n} for the advanced GF. An example for this case is shown in Fig. 3(c).

In contrast to Berezinskii’s technique for an infinite 1D system, the external vertices depend on the direction. Also, the diagrams carry a factor $\exp[2\pi i(\phi/\phi_0)(n^+ + \bar{n}^+ - n^-$

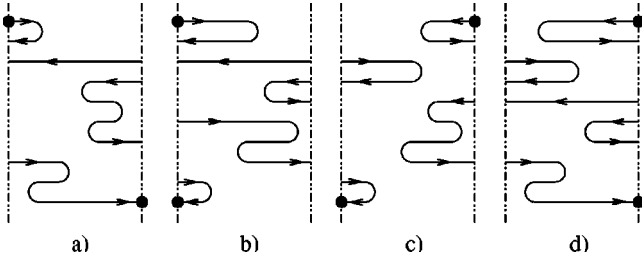


FIG. 4. The different possibilities to attach external vertices. Cases (b) and (d) contain oscillating factors $\exp[\pm 2ip(\epsilon)x]$, which is connected to the fact that the numbers of line pairs on the left- and right-hand side differ by ± 1 . Cases (a) and (c) have $m = m'$ and hence do not contain such factors.

$-\bar{n}^-]$ from the through-going lines. The number of pairs on the two sides of the cutting line, which we denote by m and m' for the retarded GF and by \bar{m} and \bar{m}' for the advanced GF, may in general differ by ± 1 (i.e., $m - m' = -1, 0, 1$ and $\bar{m} - \bar{m}' = -1, 0, 1$) as in Sec. IV. However, for $\langle G_R(\epsilon, \phi; x, x') \rangle$ in the regime of weak disorder as in Sec. III, we have always $m = m'$.

III. THE DENSITY OF STATES

The diagrams for the DOS do not exhibit the full complexity presented in the previous section, since they contain only retarded GF's. Consequently, we can omit vertices d, e, and f of Fig. 1 and set $m = m'$. Following Berezinskii's method,⁴¹ we denote the sum of all diagrams with m pairs of returning lines and $n = n^+ + n^-$ through-going lines by $Q_0(m, n; x - x' = L)$, where n^+ (n^-) is the number of right- (left-)going lines that cross the whole diagram. Such a diagram is shown in Figs. 3(a) and 3(b). Since the magnetic field dependence has been extracted from Q_0 , it only depends on the total number of through-going lines. The condition $m = m'$ restricts the possibilities to attach the external vertices to the cases (a) and (c) of Fig. 4. The average value of the retarded GF can be expressed in terms of the kernel Q_0 as

$$\begin{aligned} \langle G^+(\epsilon, \phi; x, x) \rangle = & -\frac{i}{v(\epsilon)} \sum_{m=0}^{\infty} \sum_{n^+=0}^{\infty} \sum_{n^-=0}^{\infty} \left[\binom{m+n^+}{m} \right. \\ & \times \binom{m-1+n^-}{m-1} + \binom{m+n^-}{m} \binom{m-1+n^+}{m-1} \\ & \left. - \delta_{m,0} \delta_{n^+,0} \delta_{n^-,0} \right] \exp \left\{ ip(\epsilon)L(n^+ + n^-) \right. \\ & \left. - \frac{\eta L}{v(\epsilon)}(n^+ + n^-) - 2\pi i \frac{\phi}{\phi_0}(n^+ - n^-) \right\} \\ & \times Q_0(m, n^+ + n^-; L). \end{aligned} \quad (8)$$

The two products of binomials in the square brackets of Eq. (8) characterize the different possibilities to insert the n^+ right-going and the n^- left-going lines between m pairs and correspond to the cases (a) and (c) of Fig. 4, respectively. For $m = n^+ = n^- = 0$, these two possibilities are degenerated into a pointlike diagram. To avoid double counting in this case,

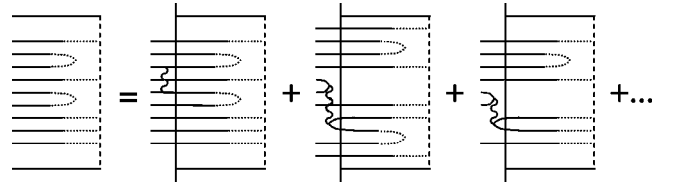


FIG. 5. How to include the internal vertices to Q_0 . Shown on the rhs is the inclusion of vertex b of Fig. 1 and the inclusion of vertex c without and with changing of m and n .

the third term in the square brackets has been added. The combinatorial factor, corresponding, e.g., to the configuration in Fig. 4(a), can be obtained as follows: n^+ lines can be distributed at $m+1$ positions, before each of the loops on the lhs and after the last loop, whereas the n^- left-going lines can be inserted at m positions before each of the loops on the rhs. Denoting the number of lines at a given position with n_i^\pm , we have the restrictions $n^+ = n_1^+ + n_2^+ + \dots + n_{m+1}^+$ and $n^- = n_1^- + n_2^- + \dots + n_m^-$.

Summing over all these possibilities gives

$$\begin{aligned} \sum_{\{n_i^+\}} \delta_{n^+, n_1^+ + n_2^+ + \dots + n_{m+1}^+} \sum_{\{n_i^-\}} \delta_{n^-, n_1^- + n_2^- + \dots + n_m^-} \\ = \binom{m+n^+}{m} \binom{m-1+n^-}{m-1}. \end{aligned} \quad (9)$$

The expression for the DOS can be obtained by combining Eqs. (2) and (8):

$$\begin{aligned} \rho(\epsilon, \phi) = \rho_0 \sum_{m=0}^{\infty} \sum_{n=0}^{\infty} \sum_{k=0}^n \left[2 \binom{m+k}{m} \binom{m+n-k-1}{m-1} \right. \\ \left. - \delta_{m,0} \delta_{n,0} \right] \cos[p(\epsilon)Ln] \\ \times \exp \left(-\frac{\eta}{v(\epsilon)}Ln \right) \cos \left(2\pi \frac{\phi}{\phi_0}(2k-n) \right) \\ \times Q_0(m, n; L). \end{aligned} \quad (10)$$

To find $Q_0(m, n; x - x')$, we shift x infinitesimally and examine the different impurity vertices that pass through the point x . The result is a differential equation for Q_0 ,

$$\begin{aligned} \frac{d}{dx} Q_0(m, n; x) = - \left[\frac{(2m+n)^2}{2l^+} + \frac{n}{2l^-} + \frac{m(m+n)}{l^-} \right] \\ \times Q_0(m, n; x) - \frac{1}{l^-} m^2 Q_0(m-1, n+2; x), \end{aligned} \quad (11)$$

where the vertices a, b, and c in Fig. 1 contribute. For vertex a the number of possibilities to be included is $2m+n$, for vertex b it is $\frac{1}{2}(2m+n)(2m+n-1)$, and to include vertex c there are $m(m+n-1)$ ways that do not change m and n and m^2 possibilities that decrease m by 1 pair and increase n by 2. The process of construction of this equation is illustrated in Fig. 5.

The kernel Q_0 satisfies the boundary condition

$$Q_0(m, n; x - x' = L = 0) = \delta_{m,0}, \quad (12)$$

which expresses the absence of scattering for a ring with infinitesimal small circumference. Equation (11) for $Q_0(m, n; x)$ can be solved exactly as shown in Appendix A:

$$\begin{aligned} Q_0(m, n; L) = & \exp \left\{ -\frac{L}{2l^+} (2m+n)^2 \right. \\ & \left. -\frac{L}{l^-} m(m+n) - \frac{L}{2l^-} n \right\} \\ & \times \sum_{j=0}^m (-1)^j \binom{m}{j} \frac{m!(j+n-2)!}{(m+j+n-1)!} \\ & \times (2j+n-1) \exp \left\{ \frac{L}{l^-} j(j+n-1) \right\}. \end{aligned} \quad (13)$$

Equations (10) and (13) give a complete description of the DOS for a one-channel ring in an external magnetic field. They are exact in the regime of weak disorder, when the condition $p_F l^\pm \gg 1$ or $\epsilon_F \tau \gg 1$ is satisfied (p_F and ϵ_F are the Fermi momentum and Fermi energy, respectively). Furthermore, since the circumference L of the ring may vary within a large range ($L \leq l^\pm$ to $l^\pm \ll L < \infty$), the results cover both the weak localization and the ballistic regimes. For the weak localization regime, when $L \gg \max(l^+, l^-)$ the amplitude of $Q_0(m, n; L)$ decreases rapidly with m and n due to the exponential prefactor. Keeping harmonics up to $n=2$ in Eq. (10) and using Eq. (A6), we obtain the leading behavior for $\rho(\epsilon, \phi)$:

$$\begin{aligned} \rho(\epsilon, \phi) = & \rho_0 \left[1 - \frac{2L}{l^-} \exp \left(-\frac{2L}{l^+} - \frac{L}{l^-} \right) \right] \\ & + 2\rho_0 \exp \left(-\frac{L}{2l^+} - \frac{L}{2l^-} \right) \\ & \times \left[\cos[p(\epsilon)L] \cos \left(2\pi \frac{\phi}{\phi_0} \right) e^{-\eta L/v(\epsilon)} \right. \\ & \left. + e^{-3L/2l^+ - L/2l^-} \cos[2p(\epsilon)L] \cos \left(4\pi \frac{\phi}{\phi_0} \right) \right] \\ & \times e^{-[2\eta/v(\epsilon)]L}. \end{aligned} \quad (14)$$

We see that the main quantum correction to the average value of the DOS oscillates with a period of ϕ_0 . The amplitude of this contribution decreases exponentially with the impurity strength or with increasing L , so that $\rho = \rho_0$ for $L \rightarrow \infty$.

The ballistic regime is realized for $L \leq \min(l^+, l^-)$. Keeping terms up to first order in m , the DOS can be approximated in this limit by

$$\begin{aligned} \rho(\epsilon, \phi) = & \rho_0(\epsilon, \phi) \\ & - \rho_0 \frac{L}{l^+} \sum_{n=0}^{N^+} n^2 \cos[p(\epsilon)Ln] \cos \left(2\pi \frac{\phi}{\phi_0} n \right) \\ & - \rho_0 \frac{L}{l^-} \sum_{n=0}^{N^-} n \cos[p(\epsilon)Ln] \cos \left(2\pi \frac{\phi}{\phi_0} n \right) \\ & - 2\rho_0 \frac{L}{l^-} \sum_{n=0}^{N^-} \sum_{k=0}^n (k+1) \cos[p(\epsilon)Ln] \\ & \times \cos \left(2\pi \frac{\phi}{\phi_0} (2k-n) \right), \end{aligned} \quad (15)$$

where $N^+ \approx [\sqrt{2l^+/L}]$ and $N^- \approx [2l^-/L]$, and the DOS of a clean ring $\rho_0(\epsilon, \phi)$ is given by Eq. (6). In the ballistic regime, L is of the same order of magnitude as l^\pm , hence N^\pm may be rather small integers. Therefore the oscillation with the full flux quantum ϕ_0 dominates in the ballistic regime.

In the absence of backward scattering ($l^- = \infty$), $Q_0(m, n; L)$ is greatly simplified:

$$Q_0(m, n; L) = \exp \left\{ -\frac{L}{2l^+} n^2 \right\} \delta_{m,0}. \quad (16)$$

Substituting Eq. (16) in (10) and using

$$\lim_{m \rightarrow 0} \binom{m+n-k-1}{m-1} = \delta_{n,k},$$

we can express the DOS as

$$\begin{aligned} \rho(\epsilon, \phi) = & \rho_0 + \frac{\rho_0}{2} \sqrt{\frac{l^+}{2\pi L}} \int_{-\infty}^{\infty} dz e^{(l^+/2L)z^2} \\ & \times \left\{ \frac{1}{\exp\{-ip(\epsilon)L - i2\pi\phi/\phi_0 + iz + [\eta/v(\epsilon)]L\} - 1} \right. \\ & \left. + \frac{1}{\exp\{-ip(\epsilon)L + i2\pi\phi/\phi_0 + iz + [\eta/v(\epsilon)]L\} - 1} + \text{c.c.} \right\}. \end{aligned} \quad (17)$$

From Eq. (17) one sees that forward scattering coherently shifts all energy levels. The value of this shifting is random with Gaussian distribution, with a typical value of $(\hbar/\tau^+) \sqrt{l^+/L}$, where τ^+ is the relaxation time due to forward scattering. The level repulsion⁴⁸ in 1D disordered systems therefore is only due to backward scattering. The width of this level broadening of the averaged system is much smaller than Dingle broadening for the weak localization regime, whereas the two mechanisms can have comparable effects in the ballistic regime.

IV. HIGHER MOMENTS OF THE DOS AND DISTRIBUTION FUNCTIONS

Exact calculations show that the average value of the DOS oscillates with a period of the flux quantum ϕ_0 . To understand the reason for the experimentally observed oscillation of the persistent current in a sufficiently large ring [$L \gg l$ (Refs. 12 and 15)] with the halved period, we calculate here higher moments of the distribution of the DOS. According to Eq. (3), we have to determine the correlators $\langle G_R^l G_A^{k-l} \rangle$ for the k th moment. In contrast to the Berezinskii technique for strictly 1D systems, the correlators here are characterized by only one block Q . An example is shown in Fig. 3(c). Each diagram contributing to $\langle G_R^l G_A^{k-l} \rangle$ consists of l retarded and $k-l$ advanced lines. For the i th retarded (advanced) GF, we count the number of left loops $m_i(\bar{m}_i)$, of right loops $m'_i(\bar{m}'_i)$, and of left- and right-going traversing

lines $n_i = n_i^+ + n_i^-$ ($\bar{n}_i = \bar{n}_i^+ + \bar{n}_i^-$). (Notice that the index i of n_i here denotes the number of the GF, whereas it was used for the position within one GF in the previous section.) For the different fermion lines, we now can attach the external vertices in four different ways, as shown in Fig. 4. This allows $m_i - m'_i = -1, 0, 1$ ($\bar{m}_i - \bar{m}'_i = -1, 0, 1$) for the each retarded (advanced) GF. It turns out that the block Q depends only on the total numbers $m = m_1 + m_2 + \dots + m_l$, $\bar{m} = \bar{m}_1 + \bar{m}_2 + \dots + \bar{m}_{k-l}$ and similarly m', \bar{m}', n, \bar{n} .⁵¹ It is clear from these considerations that the difference between m and m' is always restricted by $-l \leq m - m' \leq l$. This is automatically taken into account by the mixing coefficient⁵¹ $\varphi_l(m, m'; n^+, n^-)$. This coefficient is the generalization of the term in square brackets of Eq. (8). It counts the different possibilities to attach external vertices (see Fig. 4) and to distribute the through-going lines between the loops. Using Eq. (9), we can write it as

$$\begin{aligned} \varphi_l(m, m'; n^+, n^-) &= \sum_{\{m_i\}} \delta_{m, m_1 + m_2 + \dots + m_l} \sum_{\{m'_i\}} \delta_{m', m'_1 + m'_2 + \dots + m'_l} \sum_{\{n_i^+\}} \delta_{n^+, n_1^+ + n_2^+ + \dots + n_l^+} \sum_{\{n_i^-\}} \delta_{n^-, n_1^- + n_2^- + \dots + n_l^-} \\ &\times \prod_{i=1}^l \left\{ e^{2ip(\epsilon)x - 2\eta x/v(\epsilon)} \delta_{m_i, m'_i + 1} \binom{m_i - 1 + n_i^+}{m_i - 1} \binom{m_i - 1 + n_i^-}{m_i - 1} + e^{-2ip(\epsilon)x + 2\eta x/v(\epsilon)} \right. \\ &\times \delta_{m_i, m'_i - 1} \binom{m_i + n_i^+}{m_i} \binom{m_i + n_i^-}{m_i} + \delta_{m_i, m'_i} \left[\binom{m_i + n_i^+}{m_i} \binom{m_i - 1 + n_i^-}{m_i - 1} + \binom{m_i - 1 + n_i^+}{m_i - 1} \binom{m_i + n_i^-}{m_i} \right. \\ &\left. \left. - \delta_{m_i, 0} \delta_{n_i^+, 0} \delta_{n_i^-, 0} \right] \right\}. \end{aligned} \quad (18)$$

Separating the exponential factors in Eq. (18), we can write φ_l as

$$\varphi_l(m, m'; n^+, n^-) = e^{-2ix(m' - m)[p(\epsilon) + i\eta/v(\epsilon)]} \tilde{\varphi}_l(m, m'; n^+, n^-) \quad (19)$$

with

$$\begin{aligned} \tilde{\varphi}_l(m, m'; n^+, n^-) &= \sum_{\{m_i\}} \delta_{m, m_1 + m_2 + \dots + m_l} \sum_{\{m'_i\}} \delta_{m', m'_1 + m'_2 + \dots + m'_l} \sum_{\{n_i^+\}} \delta_{n^+, n_1^+ + n_2^+ + \dots + n_l^+} \sum_{\{n_i^-\}} \delta_{n^-, n_1^- + n_2^- + \dots + n_l^-} \\ &\times \prod_{i=1}^l \left\{ \delta_{m_i, m'_i + 1} \binom{m_i - 1 + n_i^+}{m_i - 1} \binom{m_i - 1 + n_i^-}{m_i - 1} + \delta_{m_i, m'_i - 1} \binom{m_i + n_i^+}{m_i} \binom{m_i + n_i^-}{m_i} \right. \\ &\left. + \delta_{m_i, m'_i} \left[\binom{m_i + n_i^+}{m_i} \binom{m_i - 1 + n_i^-}{m_i - 1} + \binom{m_i - 1 + n_i^+}{m_i - 1} \binom{m_i + n_i^-}{m_i} - \delta_{m_i, 0} \delta_{n_i^+, 0} \delta_{n_i^-, 0} \right] \right\}. \end{aligned} \quad (20)$$

The mixing factor for the advanced GF is obtained from complex conjugation of φ_{k-l} .

Now we can express Eq. (3) in terms of Q and the mixing factors

$$\begin{aligned} \langle \rho^k(\epsilon, \phi; L, x) \rangle &= \left(\frac{\rho_0}{2} \right)^k \sum_{l=0}^k \sum_{m=0}^k \sum_{\bar{m}=0}^{\infty} \sum_{m'=0}^{\infty} \sum_{\bar{m}'=0}^{\infty} \sum_{n^+=0}^{\infty} \sum_{n^-=0}^{\infty} \sum_{n^+=0}^{\infty} \sum_{n^-=0}^{\infty} \binom{k}{l} \\ &\times e^{-i2\pi(\phi/\phi_0)(n^+ - n^- + \bar{n}^+ - \bar{n}^-)} e^{ip(\epsilon)L(n^+ + n^- - \bar{n}^+ - \bar{n}^-)} e^{-[\eta L/v(\epsilon)](n^+ + n^- + \bar{n}^+ + \bar{n}^-)} \\ &\times e^{-2ip(\epsilon)x(m' - m - \bar{m}' + \bar{m})} e^{[2\eta x/v(\epsilon)](m' - m + \bar{m}' - \bar{m})} \\ &\times \tilde{\varphi}_l(m, m'; n^+, n^-) \tilde{\varphi}_{k-l}(\bar{m}, \bar{m}'; \bar{n}^+, \bar{n}^-) Q \left(\begin{array}{c} m, \quad m', \quad n^+ + n^- \\ \bar{m}, \quad \bar{m}', \quad \bar{n}^+ + \bar{n}^- \end{array} \middle| L \right). \end{aligned} \quad (21)$$

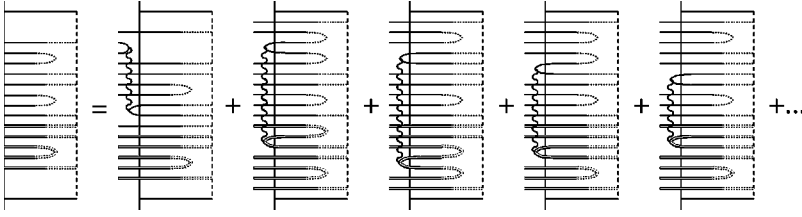


FIG. 6. Different possibilities to attach vertices to the block Q , as the left side is shifted. The first plot shows the inclusion of vertex c of Fig. 1 with decreasing m and m' by 1 and increasing n by 2. The other four blocks show the different possibilities to include vertex f and correspond to the last four terms in Eq. (22).

Here, the first three exponential factors come from the external vertices and from the revolutions around the ring. The last two exponential factors were separated from the mixing coefficients [Eq. (19)]. Below, we shall see that the last exponential factor is canceled by a contribution from Q .

Equation for the central block Q

As noted above, the central block

$$Q \left(\begin{array}{ccc} m, & m', & n \\ \bar{m}, & \bar{m}', & \bar{n} \end{array} \middle| x \right)$$

is defined as the sum of all diagrams with m and \bar{m} pairs of returning lines on the left side, m' and \bar{m}' pairs on the right side, and n and \bar{n} through-going lines, coming from retarded and advanced GF's, respectively. An equation determining Q can be constructed according to Berezinskii's idea by attaching all possible vertices, given in Fig. 1, to the existing block, while avoiding the formation of unconnected electron loops. Careful analysis of all these possibilities gives the equation

$$\begin{aligned} \frac{d}{dx} Q \left(\begin{array}{ccc} m & m' & n \\ \bar{m} & \bar{m}' & \bar{n} \end{array} \middle| x \right) = & - \left[\frac{1}{2l^+} (2m+n-2\bar{m}-\bar{n})^2 + \frac{1}{l^-} m(m+n) + \frac{1}{l^-} \bar{m}(\bar{m}+\bar{n}) + \frac{1}{2l^-} (n+\bar{n}) \right] Q \left(\begin{array}{ccc} m & m' & n \\ \bar{m} & \bar{m}' & \bar{n} \end{array} \middle| x \right) \\ & - \frac{1}{l^-} mm' Q \left(\begin{array}{ccc} m-1 & m'-1 & n+2 \\ \bar{m} & \bar{m}' & \bar{n} \end{array} \middle| x \right) - \frac{1}{l^-} \bar{m} \bar{m}' Q \left(\begin{array}{ccc} m & m' & n \\ \bar{m}-1 & \bar{m}'-1 & \bar{n}+2 \end{array} \middle| x \right) \\ & + \frac{1}{l^-} m \bar{m} e^{4\eta x/v(\epsilon)} Q \left(\begin{array}{ccc} m-1 & m' & n \\ \bar{m}-1 & \bar{m}' & \bar{n} \end{array} \middle| x \right) + \frac{1}{l^-} (m+n)(\bar{m}+\bar{n}) e^{-4\eta x/v(\epsilon)} Q \left(\begin{array}{ccc} m+1 & m' & n \\ \bar{m}+1 & \bar{m}' & \bar{n} \end{array} \middle| x \right) \\ & + \frac{1}{l^-} m'(\bar{m}+\bar{n}) e^{-4\eta xv(\epsilon)} Q \left(\begin{array}{ccc} m & m'-1 & n+2 \\ \bar{m}+1 & \bar{m}' & \bar{n} \end{array} \middle| x \right) + \frac{1}{l^-} (m+n)\bar{m}' e^{-4\eta x/v(\epsilon)} \\ & \times Q \left(\begin{array}{ccc} m+1 & m' & n \\ \bar{m} & \bar{m}'-1 & \bar{n}+2 \end{array} \middle| x \right) + \frac{1}{l^-} m' \bar{m}' e^{-4\eta x/v(\epsilon)} Q \left(\begin{array}{ccc} m & m'-1 & n+2 \\ \bar{m} & \bar{m}'-1 & \bar{n}+2 \end{array} \middle| x \right). \end{aligned} \quad (22)$$

The block Q is subjected to a similar boundary condition as Q_0 in the previous section,

$$Q \left(\begin{array}{ccc} m & m' & n \\ \bar{m} & \bar{m}' & \bar{n} \end{array} \middle| x=0 \right) = \delta_{m,0} \delta_{m',0} \delta_{\bar{m},0} \delta_{\bar{m}',0}, \quad (23)$$

which states that for an infinitesimal ring there can be no scattering. The first coefficient on the right hand side of Eq. (22) contains contributions from the vertices a, a' , b, b' , c, c' , and d in Fig. 1. Vertices a , b , and d can be attached in $(2m+n)$, $\frac{1}{2}(2m+n)(2m+n-1)$, and $(2m+n)(2\bar{m}+\bar{n})$ ways, respectively, the coefficients for a' and b' are the same as for a and b , with the replacement $\{m, n\} \rightarrow \{\bar{m}, \bar{n}\}$. For vertex c we have again to distinguish two possibilities as in Sec. III. We have $m(m+n-1)$ ways to attach it without changing m, m' , and n ; and mm' different ways with chang-

ing $\{m, m', n\} \rightarrow \{m-1, m'-1, n+2\}$. The latter kind of insertion of the vertex c in Fig. 1 and its counterpart for the advanced GF give the second and the third term on the right-hand side of Eq. (22). The inclusion of vertex e reduces m and \bar{m} by 1. The insertion of vertex f , however, can be done in four different ways that are shown schematically in the last four blocks of Fig. 6.

Trying to solve Eq. (22), one may begin by substituting $\tilde{Q} = Q/(m'!\bar{m}'!)$ and then introduce new variables $M = 2m+n$, and $\bar{M} = 2\bar{m}+\bar{n}$, $M' = 2m'+n$, and $\bar{M}' = 2\bar{m}' + \bar{n}$. As a consequence, M' and \bar{M}' appear as fixed parameters in the differential equation for \tilde{Q} . But still then, \tilde{Q} depends on the five variables M, n, \bar{M}, \bar{n} , and x . Under these circumstances, looking for the general analytic solution of Eq. (22), one meets with enormous difficulties. Before study-

ing an asymptotic approximation of the problem, we make some simplifications of Eqs. (21) and (22). The exponential factors in Eq. (22) can be removed by the following substitution:

$$Q \begin{pmatrix} m & m' & n \\ \bar{m} & \bar{m}' & \bar{n} \end{pmatrix} x = \exp \left\{ \frac{2\eta x}{v(\epsilon)} (m + \bar{m} - m' - \bar{m}') \right\} \times \bar{Q} \begin{pmatrix} m & m' & n \\ \bar{m} & \bar{m}' & \bar{n} \end{pmatrix} x. \quad (24)$$

The equation for \bar{Q} has the same structure as Eq. (22), only the exponential factors are dropped and the first term on the rhs of Eq. (22) acquires another contribution $-[2\eta/v(\epsilon)](m + \bar{m} - m' - \bar{m}')$ to the prefactor of Q .

From the structure of the internal vertices in Fig. 1 one sees that the condition

$$(m' - m) - (\bar{m}' - \bar{m}) = 0 \quad (25)$$

is satisfied for arbitrary cross sections. (The same condition also applies to the strictly 1D problem; see Ref. 51.) A corresponding symmetry of Eq. (22) confirms this condition.

In the regime of weak disorder, $p_F l \gg 1$, Eq. (21) for the k th moment of the DOS contains terms that strongly oscillate with the particle energy ($n^+ + n^- \neq \bar{n}^+ + \bar{n}^-$) apart from smooth ones ($n^+ + n^- = \bar{n}^+ + \bar{n}^-$). To neglect the strongly oscillating terms, we choose only those terms in Eq. (21) that satisfy the condition

$$n^+ + n^- = \bar{n}^+ + \bar{n}^-. \quad (26)$$

Equation (21) now is simplified to

$$\begin{aligned} & \langle \rho^k(\epsilon, \phi; L) \rangle \\ &= \left(\frac{\rho_0}{2} \right)^k \sum_{m=0}^{\infty} \sum_{\bar{m}=0}^{\infty} \sum_{m'=0}^{\infty} \sum_{\bar{m}'=0}^{\infty} e^{i4\pi(\phi/\phi_0)n - [2\eta L/v(\epsilon)]n} \\ & \times \bar{Q} \begin{pmatrix} m & m' & n \\ \bar{m} & \bar{m} - m + m' & \bar{n} \end{pmatrix} x \\ & \times \Phi_k(m, \bar{m}, m', \bar{m}' - m + m', n, \bar{n}), \end{aligned} \quad (27)$$

where

$$\begin{aligned} & \Phi_k(m, \bar{m}, m', \bar{m}', n, \bar{n}) \\ &= \sum_{l=0}^k \sum_{n^+=0}^n \sum_{\bar{n}^+=0}^{\bar{n}} \binom{k}{l} \\ & \times e^{-i4\pi(\phi/\phi_0)(n^+ + \bar{n}^+)} \\ & \times \tilde{\varphi}_l(m, m'; n^+, n - n^+) \\ & \times \tilde{\varphi}_{k-l}(\bar{m}, \bar{m}'; \bar{n}^+, \bar{n} - \bar{n}^+). \end{aligned} \quad (28)$$

Expressions (27) and (28) show that the dominating contribution to $\langle \rho^k \rangle$ does not strongly oscillate with the energy. Unlike the averaged DOS, the first harmonic of all moments

oscillates with the halved magnetic flux $\phi_0/2$. In the following section, we solve Eqs. (20)–(28) for large rings, with $L \gg \max\{l^+, l^-\}$.

V. DISTRIBUTION FUNCTIONS FOR THE WEAK LOCALIZATION LIMIT

The equation for \bar{Q} is simplified considerably in the limit of large rings, $L \gg \max\{l^+, l^-\}$. For this case, we can assume that the electrons are quasilocalized and that the wave function overlaps around the ring are small, similar to a tight-binding model. Diagrammatically, this means that the electron loops emerging from the lhs and the rhs of the diagram almost never reach each other, since they have a characteristic size of $\xi \ll L$. (The localization length for an infinite 1D system is^{41,42} $\xi_{1D} \sim 4l^-$.)

As a consequence, we can for large rings neglect those inclusions of the vertices c, c', e, and f that directly connect the loops on the rhs with those on the lhs. Corresponding to this is the neglect of the terms 2, 3, and 6–10 on the rhs of Eq. (22). Now, \bar{Q} can be factored as

$$\begin{aligned} & \bar{Q} \begin{pmatrix} m & m' & n \\ \bar{m} & \bar{m} - m + m' & \bar{n} \end{pmatrix} x \\ &= Q^*(m, \bar{m}, n; x) Q^*(m', \bar{m} - m + m', n; x), \end{aligned} \quad (29)$$

where the factors are defined through

$$\begin{aligned} \frac{dQ^*(m, \bar{m}, n; x)}{dx} &= - \left[\frac{2\eta}{v(\epsilon)} (m + \bar{m}) + \frac{2}{l^+} (m - \bar{m})^2 \right. \\ & \left. + \frac{1}{l^-} m(m+n) + \frac{1}{l^-} \bar{m}(\bar{m} + \bar{n}) + \frac{1}{l^-} n \right] \\ & \times Q^*(m, \bar{m}, n; x) + \frac{1}{l^-} m\bar{m} \\ & \times Q^*(m-1, \bar{m}-1, n; x) + \frac{1}{l^-} (m+n) \\ & \times (\bar{m} + \bar{n}) Q^*(m+1, \bar{m}+1, n; x). \end{aligned} \quad (30)$$

Apart from this simplification, the limit $L \gg \max\{l^+, l^-\}$ implies $m, \bar{m}, m' \gg n$.

Note that Eq. (30) can also be obtained from Eqs. (22) and (24) by neglecting m' and \bar{m}' . The nonentanglement mentioned above has a second consequence: The remaining contributions change m and \bar{m} simultaneously by ± 1 (due to vertices e and f of Fig. 1), or conserve both m and \bar{m} , as in Berezinskii's approach to strictly 1D systems.⁴¹ Therefore we can adopt $m = \bar{m}$, which further simplifies Eq. (30):

$$\begin{aligned}
& l^{-} \frac{dQ^*(m,n;x)}{dx} \\
&= -[4\eta\tau^{-}m+n+2m(m+n)]Q^*(m,n;x) \\
&\quad + m^2Q^*(m-1,n;x) + (m+n)^2Q^*(m+1,n;x).
\end{aligned} \tag{31}$$

Here, τ^{-} is the inelastic scattering time with respect to backward scattering. The boundary condition for Eq. (31) is

$$Q^*(m,n;x=0) = \delta_{m,0}. \tag{32}$$

The combined mixing function Φ_k given in Eq. (28) is simplified for large m , \bar{m} , and m' in Appendix B. Substituting Eqs. (B6) and (29) into (27), we get a comparatively simple expression for $\langle \rho^k \rangle$:

$$\begin{aligned}
\langle \rho^k(\epsilon, \phi; L) \rangle &= \left(\frac{\rho_0}{2} \right)^k \sum_{m=0}^{\infty} \sum_{m'=0}^{\infty} \sum_{n=0}^{\infty} \sum_{l=0}^k \left[\cos \left(2\pi \frac{\phi}{\phi_0} \right) \right]^{2n} \\
&\quad \times e^{-[2\eta L/v(\epsilon)]n} \binom{k}{l} \binom{2l}{m-m'} \binom{2k-2l}{m-m'} \\
&\quad \times \frac{2^{2n} m^{k+2n-2}}{\Gamma(l)\Gamma(k-l)} Q^*(m,n;L) Q^*(m',n;L).
\end{aligned} \tag{33}$$

As we emphasized, the diagrammatical structure of the block Q^* demands its dependence on one parameter m instead of two (m and \bar{m}). Hereby the sum over \bar{m} is removed. The summations over l and m' can be done as described in Appendix B. Using Eqs. (B7) and (B8), we get

$$\begin{aligned}
\langle \rho^k(\epsilon, \phi; L) \rangle &= \rho_0^k \frac{2^{1-k}(k-1)}{k(2k-1)} \frac{\Gamma^2(2k)}{\Gamma^5(k)} \\
&\quad \times \sum_{n=0}^{\infty} \sum_{m=0}^{\infty} \frac{2^{2n} e^{-[2\eta L/v(\epsilon)]n} m^{k+2n-2}}{\Gamma^2(n+1)} \\
&\quad \times \left[\cos \left(2\pi \frac{\phi}{\phi_0} \right) \right]^{2n} Q^{*2}(m,n;L)
\end{aligned}$$

$$\begin{aligned}
&= \langle \rho^k(\epsilon, \phi; L) \rangle_{n=0} + \langle \rho^k(\epsilon, \phi; L) \rangle_{n=1} \\
&\quad \times \cos^2 \left(\frac{2\pi\phi}{\phi_0} \right) + \dots
\end{aligned} \tag{34}$$

Equation (31) for $Q^*(m,n;x)$ was solved approximately in Ref. 52 for arbitrary n . Here we shall study this equation for the zeroth and first harmonics ($n=0$ and $n=1$) in detail.

A. Zeroth harmonic contribution to the DOS moments

The zeroth harmonic of $\langle \rho^k(\epsilon, \phi; L) \rangle$ in Eq. (34) contains $Q^*(m,n=0;L)$. By performing a Laplace transform of Eq. (31), written for $n=0$, with respect to x and using the boundary condition (32), we get

$$\begin{aligned}
& (\lambda + s_1 m) Q_0^*(m; \lambda) - \delta_{m,0} \\
&= m^2 [Q_0^*(m+1; \lambda) + Q_0^*(m-1; \lambda) - 2Q_0^*(m; \lambda)].
\end{aligned} \tag{35}$$

Here, $s_1 = 4\eta\tau^{-}$ and λ is the parameter of the Laplace transform. This is an equation for the right-hand side in the Berezinskii technique with an open boundary condition and it was solved in Refs. 53 and 51. Here, we give only the result for $Q_0^*(s_1, m; x)$:

$$\begin{aligned}
Q_0^*(s_1, m; x) &= 2(ms_1)^{1/2} K_1(2(ms_1)^{1/2}) \\
&\quad + \frac{2(ms_1)^{1/2}}{2\pi i} \int_{-\infty}^{\infty} d\lambda \frac{s_1^{-(1+i\lambda)/2} \Gamma^3\left(\frac{1-i\lambda}{2}\right)}{i-\lambda} \frac{1}{\Gamma^2(-i\lambda)} \\
&\quad \times e^{-(\lambda^2+1)(x/4l^-)} K_{-i\lambda}(2(ms_1)^{1/2}).
\end{aligned} \tag{36}$$

After substitution of this solution into $\langle \rho^k(\epsilon, \phi; L) \rangle_{n=0}$ in Eq. (34), the summation over m can be transformed into an integration, which is done easier. Some mathematics results in the following form of $\langle \rho^k(\epsilon, \phi; L) \rangle_{n=0}$:

$$\begin{aligned}
\langle \rho^k(\epsilon, \phi; L) \rangle_{n=0} &= \left(\frac{\rho_0}{2} \right)^k \frac{2(k-1)\Gamma(2k)}{k(2k-1)\Gamma^5(k)} s_1^{1-k} \left\{ \frac{k}{k-1} \Gamma^4(k) + \frac{2}{\sqrt{s_1}} e^{-L/4} \int_{-\infty}^{\infty} \frac{d\lambda}{2\pi i} \frac{e^{-(L/4l^-)(\lambda-i\gamma)^2 - (L/4l^-)\gamma^2}}{i-\lambda} \right. \\
&\quad \times \frac{\Gamma^3\left(\frac{1-i\lambda}{2}\right)}{\Gamma^2(-i\lambda)} \left| \Gamma\left(\frac{2k+1+i\lambda}{2}\right) \Gamma\left(\frac{2k-1+i\lambda}{2}\right) \right|^2 + \frac{2}{s_1} \int_{-\infty}^{\infty} \frac{dz'}{2\pi i} e^{-(L/2l^-)z'^2} |\Gamma(k-iz')|^2 \\
&\quad \times \int_{-\infty}^{\infty} \frac{dz}{2\pi i} \frac{e^{-(L/2l^-)(z-i\gamma)^2 - (L/2l^-)\gamma^2 - L/2l^-}}{(z+z'-i)(z-z'-i)} \frac{\Gamma^3\left(\frac{1-iz-iz'}{2}\right) \Gamma^3\left(\frac{1-iz+iz'}{2}\right)}{\Gamma^2(-iz-iz')\Gamma^2(-iz+iz')} |\Gamma(k-iz)|^2 \left. \right\}, \tag{37}
\end{aligned}$$

where $\gamma=(l^-/L)\ln(1/s_1)>0$. The second term in the curly brackets of Eq. (37) has a saddle point at $\lambda_0=i\gamma$ and simple poles at the upper half plane: $\lambda_1=i$, $\lambda_2=i(2k-1)$, $i(2k+1)$, \dots . The integral over z in the third term in the curly brackets contains again the saddle point at $z_0=i\gamma$ and poles at $z_1=\pm z'+i$, $z_2=ik$, $i(k+1)$, \dots . For $\gamma<1$, the main contribution to both integrals is given by the saddle points. As a result we get

$$\langle \rho^k(\epsilon, \phi; L) \rangle_{n=0} = \rho_0^k (2s_1)^{1-k} \frac{\Gamma(2k-1)}{\Gamma(k)}. \quad (38)$$

Such a result has been obtained for the infinite 1D disordered system.⁵¹ Transforming the semi-invariants in Eq. (38) to moments and using the inverse Mellin transformation

$$W(\rho) = \frac{1}{2\pi i} \int_{a-i\infty}^{a+i\infty} \frac{dk}{\rho^{k+1}} \langle \rho^k \rangle, \quad (39)$$

the following inverse Gaussian distribution function is obtained:

$$W_{n=0}(\rho) = \left(\frac{2\eta\tau^- \rho_0}{\pi\rho^3} \right)^{1/2} \exp\left(-2 \frac{(\rho-\rho_0)^2}{\rho\rho_0} \eta\tau^- \right). \quad (40)$$

For $2\eta\tau^- \gg 1$, the most probable or typical value of ρ is equal to ρ_0 , whereas for $2\eta\tau^- \ll 1$ it shifts to lower values and becomes equal to $\rho_{\text{typ}} = (4\eta\tau^-/3)\rho_0$.

When γ assumes intermediate values, i.e., $1 < \gamma < k$, the essential contribution to $\langle \rho^k \rangle_{n=0}$ comes from the saddle points of the third term in the curly brackets of Eq. (37) and the contributions from the poles of this term cancel the other term, resulting in

$$\langle \rho^k(\epsilon, \phi; L) \rangle_{n=0} = \frac{\rho_0^k \Gamma(2k-1)}{2^{k-1} \Gamma(k-1) \Gamma(k+1)} \frac{s_1^{-k} l^- e^{-(L/2l^-)(1+\gamma^2)} \Gamma^6\left(\frac{1+\gamma}{2}\right)}{\pi L (1-\gamma)^2 \Gamma^4(\gamma)} \Gamma(k+\gamma) \Gamma(k-\gamma). \quad (41)$$

This expression shows that high moments of the DOS for intermediate values of γ increase with k ; however, the increase is not so rapid, as Eq. (41) has an additional factor $1/k!$ compared to Eq. (38).

For γ satisfying the condition $\gamma < k$, the leading contribution is given by the pole $z_2=ik$ and

$$\langle \rho^k(\epsilon, \phi; L) \rangle_{n=0} = \left(\frac{\rho_0}{2} \right)^k \sqrt{\frac{l^-}{2\pi L k(k-1)(2k-1)}} \frac{\Gamma^2(2k)}{\Gamma^7(k)} \Gamma^6\left(\frac{k+1}{2}\right) e^{(L/2l^-)(k^2-1)}. \quad (42)$$

The last expression is valid for arbitrary small values of the dissipation parameter ($\eta \rightarrow 0$ or $\gamma \rightarrow \infty$) with $\eta \ll (1/4\tau^-) \exp(-kL/l^-)$. Equation (42) shows that the zeroth harmonic of the k th moment of the DOS grows with k as $\exp(k^2)$. Such rapid increasing of high moments of $\langle \rho^k \rangle_{n=0}$ has been firstly obtained by Wegner⁴⁶ and it is a characteristic feature of the logarithmic normal distribution of $\langle \rho^k \rangle_{n=0}$. The distribution function for the zeroth harmonic term can be obtained using Eq. (39). For large values of the DOS, satisfying the condition $\rho > (\rho_0/2) \exp(L/l^-)$, the dominating saddle point yields again a logarithmic normal distribution:

$$W_{n=0}(\rho) = \frac{8l^-}{\pi\rho_0 L} \frac{\Gamma\left(\frac{2l^-}{L} \ln \frac{2\rho}{\rho_0} - 2\right) \Gamma\left(\frac{2l^-}{L} \ln \frac{2\rho}{\rho_0}\right) \Gamma^6\left(\frac{1}{2} + \frac{l^-}{2L} \ln \frac{2\rho}{\rho_0}\right)}{\Gamma\left(\frac{l^-}{L} \ln \frac{2\rho}{\rho_0} + 1\right) \Gamma^6\left(\frac{l^-}{L} \ln \frac{2\rho}{\rho_0}\right)} \exp\left[-\frac{l^-}{2L} \left(\ln \frac{2\rho}{\rho_0} + \frac{L}{l^-} \right)^2 \right]. \quad (43)$$

For small values of ρ , when $\rho < (\rho_0/2) \exp(L/l^-)$, the main contribution comes from the pole at the origin and the distribution function decreases in a powerlike form:

$$W_{n=0}(\rho) = \frac{2\rho_0}{\rho^2} \sqrt{\frac{l^-}{2\pi L}}. \quad (44)$$

Thus the distribution function for the zeroth harmonic or ϕ -independent component has asymmetric form.

B. Amplitude of the first harmonic contribution to the DOS moments

By a Laplace transform with respect to x , Eq. (31) with $n=1$ is converted to

$$\begin{aligned} & (\lambda + s_1 m) Q_1^*(m; \lambda) - \delta_{m,0} \\ & = (m+1)^2 [Q_1^*(m+1; \lambda) - Q_1^*(m; \lambda)] \\ & \quad + m^2 [Q_1^*(m-1; \lambda) - Q_1^*(m; \lambda)]. \end{aligned} \quad (45)$$

The δ symbol on the left-hand side of this equation comes from the boundary condition (32). Equation (45) corresponds to the equation for the central part in the Berezinskii technique for strictly 1D systems with open boundary.⁵³ For $m \gg 1$, this equation is transformed into a differential equation,

$$m^2 \frac{d^2 Q_1^*(m; \lambda)}{dm^2} + 2m \frac{dQ_1^*(m; \lambda)}{dm} - (\lambda + s_1 m) Q_1^*(m; \lambda) = 0. \quad (46)$$

A change of the function to $(1/z)\Phi(z,\lambda)=Q_1^*(m;\lambda)$, where $z^2=4ms_1$, reduces Eq. (46) to the Bessel equation

$$\frac{d^2\Phi}{dz^2} + \frac{1}{z} \frac{d\Phi}{dz} - \left(1 + \frac{1+4\lambda}{z^2}\right)\Phi = 0. \quad (47)$$

Therefore $Q_1^*(m;\lambda)$ can be expressed as

$$Q_1^*(m;\lambda) = C \frac{1}{2(m s_1)^{1/2}} K_{1+2q}(2(m s_1)^{1/2}), \quad (48)$$

where $q = -\frac{1}{2} + \sqrt{\lambda + \frac{1}{4}}$.

Equation (48) contains an unknown parameter C due to the neglect of the Kronecker symbol in Eq. (45).

On the other hand Eq. (45) has been solved by Melnikov,⁵³ who obtained the asymptotic solution of $Q_1^*(m;\lambda)$ for $1 \ll m \ll s_1^{-1}$ as

$$Q_1^*(m;\lambda) = \frac{\Gamma^3(q+1)}{\Gamma(2q+2)} m^{-q-1}. \quad (49)$$

The comparison of Eq. (48) with the asymptotic form (49) allows us to determine C :

$$C = 4s_1^{q+1} \frac{\Gamma^3(q+1)}{\Gamma(2q+2)\Gamma(2q+1)}. \quad (50)$$

Taking the inverse Laplace transform, one obtains for $Q_1^*(m;x)$

$$Q_1^*(m;x) = \int_{-\infty}^{\infty} \frac{d\lambda}{2\pi} e^{-(1/4)(\lambda^2+1)(x/l^-)} s_1^{(1-i\lambda)/2} (m s_1)^{-1/2} K_{-i\lambda}(2(m s_1)^{1/2}) \frac{\Gamma^3\left(\frac{1-i\lambda}{2}\right)}{\Gamma^2(-i\lambda)}. \quad (51)$$

To get an expression for the first harmonic, $\langle \rho^k(\epsilon, L) \rangle_{n=1}$, we substitute the solution (51) into Eq. (34), and sum over m , which can be done after the transformation of the sum into an integral over $\kappa = m s_1$:

$$\begin{aligned} \langle \rho^k(\epsilon, L) \rangle_{n=1} &= \left(\frac{\rho_0}{2}\right)^k \frac{(k-1)\Gamma(2k)}{k\Gamma^5(k)} s_1^{-k} e^{-L/2l^-} \int_{-\infty}^{\infty} \frac{d\lambda}{2\pi} s_1^{-i\lambda/2} e^{-(L/4l^-)\lambda^2} \frac{\Gamma^3\left(\frac{1-i\lambda}{2}\right)}{\Gamma^2(-i\lambda)} \\ &\times \int_{-\infty}^{\infty} \frac{d\lambda'}{2\pi} s_1^{-i\lambda'/2} e^{-(L/4l^-)\lambda'^2} \frac{\Gamma^3\left(\frac{1-i\lambda'}{2}\right)}{\Gamma^2(-i\lambda')} \left| \Gamma\left(k + \frac{i\lambda + i\lambda' - 1}{2}\right) \Gamma\left(k + \frac{i\lambda - i\lambda' - 1}{2}\right) \right|^2. \end{aligned} \quad (52)$$

For convenience, we substitute below the variables λ and λ' by z and z' according to $\lambda = z + z'$ and $\lambda' = z - z'$.

The values of the integrals in Eq. (52) are determined by saddle points and poles. For $\gamma = (l^-/L)\ln(1/s_1) < k - \frac{1}{2}$, the contribution from the saddle point dominates:

$$\langle \rho^k(\epsilon, L) \rangle_{n=1} = \left(\frac{\rho_0}{2}\right)^k \frac{(k-1)l^- \Gamma^2(2k) s_1^{-k}}{k\pi L \Gamma^5(k)} e^{-(L/2l^-)(1+\gamma^2)} \frac{\Gamma^2\left(\frac{2k-1}{2}\right) \Gamma^6\left(\frac{1+\gamma}{2}\right) \Gamma\left(\frac{2k-1+2\gamma}{2}\right) \Gamma\left(\frac{2k-1-2\gamma}{2}\right)}{\Gamma^4(\gamma)}. \quad (53)$$

For $\gamma > k - \frac{1}{2}$ the main contribution is given by the pole at $z = i(k - \frac{1}{2})$ and one gets

$$\langle \rho^k(\epsilon, L) \rangle_{n=1} = \left(\frac{\rho_0}{2}\right)^k \frac{2(k-1)\Gamma(2k)\Gamma(2k-1)\Gamma^6\left(\frac{2k+1}{4}\right)}{k\Gamma^5(k)\Gamma^2\left(\frac{2k-1}{2}\right)} \sqrt{\frac{l^-}{2\pi L s_1}} e^{(L/8l^-)(2k-1)^2 - L/2l^-}. \quad (54)$$

In contrast to the expression of $\langle \rho^k(\epsilon, L) \rangle_{n=0}$ for small dissipation, $\eta \rightarrow 0$ [see Eq. (42)], the expression for $\langle \rho^k(\epsilon, L) \rangle_{n=1}$ increases strongly with $s_1 = 4\tau^- \eta \rightarrow 0$. It is illustrative to rewrite the prefactor of Eq. (54) as $[2\pi(L/l^-)s_1]^{-1/2} = (8\pi^2\eta/\Delta)^{-1/2}$ in terms of the level distance $\Delta = 1/\rho_0 L$ and the dissipation energy η , the latter blurring the quantized energy levels. By decreasing η , the energy levels are sharpened and the distribution function becomes a δ function.

Substituting Eq. (54) into (39), one receives a normal logarithmic distribution for $\rho > (\rho_0/2)\exp(-L/l^-)$:

$$W_{n=1}(\rho) = \frac{l^-}{\pi L} \sqrt{\frac{2}{s_1 \rho \rho_0}} \frac{\Gamma\left(1 + \frac{2l^-}{L} \ln \frac{2\rho}{\rho_0}\right) \Gamma\left(\frac{2l^-}{L} \ln \frac{2\rho}{\rho_0}\right) \Gamma^6\left(\frac{1}{2} + \frac{l^-}{2L} \ln \frac{2\rho}{\rho_0}\right)}{\Gamma\left(\frac{3}{2} + \frac{l^-}{L} \ln \frac{2\rho}{\rho_0}\right) \Gamma\left(\frac{l^-}{L} \ln \frac{2\rho}{\rho_0} - \frac{1}{2}\right) \Gamma^3\left(\frac{l^-}{L} \ln \frac{2\rho}{\rho_0} + \frac{1}{2}\right) \Gamma^2\left(\frac{l^-}{L} \ln \frac{2\rho}{\rho_0}\right)} \exp\left[-\frac{l^-}{2L} \left(\ln \frac{2\rho}{\rho_0} + \frac{L}{l^-}\right)^2\right]. \quad (55)$$

The logarithmic normal distribution function for the first harmonic is valid for a large range of ρ . Comparing Eq. (55) with Eq. (43) for winding number zero, it can be seen that Eq. (55) contains in addition a prefactor $\sqrt{\rho_0/\eta\tau^-}\rho = (\pi\eta l^- \rho)^{-1}$, which increases with decreasing temperature. Thus the first harmonic increases with decreasing temperature faster in amplitude than the zeroth harmonic.

VI. CONCLUSION

The distribution function for the local DOS in a one-channel ring threaded by a magnetic flux through the opening was studied in this paper. For this purpose, we constructed a diagrammatic method as an extension of the Berezinskii technique⁴¹ to the problem with periodic boundary conditions and in the presence of an external magnetic field. The equations obtained [Eqs. (10)–(12) and (21)–(23) for the DOS and its k th moments, respectively] are exact in the framework of the weak disorder limit $k_F l \gg 1$. Equations (11) and (12) are solved exactly, which gives the oscillation of ρ with the full flux for both weak localization and ballistic regimes.

In contrast to the DOS problem, the equation for $\langle \rho^k(\epsilon, \phi; L) \rangle$ is rather complicated and we succeeded to solve it for the weak localization limit when $L \gg l^\pm$. In this limit, the leading contributions to arbitrary moments of the DOS oscillate with the halved period $\phi_0/2$. The distribution functions for zeroth (insensitive to the magnetic field) and first (with a period of $\phi_0/2$) harmonics are calculated and logarithmic normal distributions [Eqs. (43) and (55)] are obtained for them, indicating large contributions from high moments of the DOS. For the zeroth harmonic, this normal logarithmic shape appears for the tail of the distribution, but for the first harmonic it covers the large range of $\rho > (\rho_0/2)\exp(-L/l^-)$, i.e., the high moments give essential contributions not only on the tail but also in the vicinity of the average value of the DOS. The distribution function for the first harmonic increases with decreasing the width of the energy levels or the dissipation parameter η [see Eq. (55)], which was introduced phenomenologically in the theory [Eq. (4)]. For $\eta \rightarrow 0$, the distribution function $W_{n=1}(\rho)$ becomes a δ function due to the quantization of the energy levels in the rings. The results for the DOS show that the amplitudes of all harmonics of $\rho(\epsilon, \phi)$ are exponentially small in the weak localization regime [Eq. (14)], while the amplitudes of the higher moments in this regime [Eqs. (38), (41), (42), and (54)] are relatively large. Although we could not calculate higher moments of the DOS in the ballistic regime, the amplitude of the average value of the DOS is large and seems to be consistent with experimental data.¹⁴

It is also well known that the DOS of 1D disordered crys-

talline systems is very sensitive to the filling factor. There exists disorder induced enhancement of the DOS for commensurable values of the electron wavelength λ and the lattice constant a , when the electronic energy ϵ satisfies the condition $p(\epsilon) = k\pi/na$, $k = \pm 1, \pm 2, \dots, \pm n$ and $n = 2, 3, \dots$, and the effect is pronounced for half filling which corresponds to $n = 2$. The singularity in the DOS of 1D disordered crystalline systems near the middle of the band is known as a Dyson singularity⁵⁴ which was studied for many 1D electronic models.^{55–60} Notice that the Berezinskii method has also been applied to study the conductivity and the localization length^{60,42} apart from the Dyson singularity in the middle of the band of a 1D infinite lattice with both weak and strong disorder.^{60,61} Our preliminary study shows that the real space diagrammatic method presented in this paper is applicable to study the Dyson singularity in the DOS of a ring for a half-filled energy band. This leads to a remarkable high amplitude of the persistent current as it is observed in the experiments, provided that the Peierls transition is suppressed by impurities and by weak transvers tunneling between the channels.

ACKNOWLEDGMENTS

The authors thank M. Kiselev for discussion. This work was supported by the SFB410.

APPENDIX A: SOLUTION FOR $Q_0(m, n; x)$

The first term on the right hand side of Eq. (11) can be removed through the transformation

$$Q_0(m, n; x) = \exp\left\{-\frac{x}{2l^+}(2m+n)^2 - \frac{x}{2l^-}n - \frac{x}{l^-}m(m+n)\right\} Q_0^*(m, n; x), \quad (A1)$$

which gives for Eqs. (11) and (12) the simpler form

$$l^- \frac{dQ_0^*(m, n; x)}{dx} = -m^2 \exp\left\{\frac{xn}{l^-}\right\} Q_0^*(m-1, n+2; x)$$

with

$$Q_0^*(m, n; x=0) = \delta_{m,0}. \quad (A2)$$

Laplace transformation from x to λ yields

$$\lambda \overline{Q_0}(m, n; \lambda) - \delta_{m,0} = -\frac{1}{l^-} m^2 \overline{Q_0}\left(m-1, n+2; x - \frac{n}{l^-}\right). \quad (A3)$$

Equation (A3) can be solved by iteration:

$$\overline{Q}_0(m,n;\lambda) = \left(\frac{-1}{l^-}\right)^m (m!)^2 \prod_{j=0}^m \frac{1}{\lambda - (1/l^-)j(j+n-1)} = \frac{(m!)^2}{\lambda} \frac{\Gamma\left(z+1+\frac{n-1}{2}\right)\Gamma\left(\frac{n-1}{2}+1-z\right)}{\Gamma\left(\frac{n-1}{2}+m+1+z\right)\Gamma\left(\frac{n-1}{2}+m+1-z\right)}, \quad (\text{A4})$$

where $z^2 = \lambda l^- + (n-1)^2/4$. The inverse Laplace transform gives for Q_0^*

$$Q_0^*(m,n;x) = (m!)^2 \sum_{j=0}^m \exp\left\{\frac{x}{l^-}j(j+n-1)\right\} \frac{(-1)^j}{j!(m-j)!} \frac{(j+n-2)!}{(m+j+n-1)!} (2j+n-1), \quad (\text{A5})$$

which, in connection with Eq. (A1), gives the final result, Eq. (13), where x is replaced by the full circumference L . The compliance of Eq. (A5) with the boundary condition is easily checked. Also, for $m=0$, $Q_0^*(0,n;x)=1$, and for $n=0$ we get from the inverse Laplace transform of Eq. (A4) or from taking the limit of Eq. (A5),

$$Q_0^*(m,0;x) = \left(1 - m - m \frac{x}{l^-}\right) + \sum_{j=2}^m \exp\left\{\frac{x}{l^-}j(j+n-1)\right\} \binom{m}{j} (-1)^j \frac{m!(j+n-2)!}{(m+j+n-1)!} (2j+n-1). \quad (\text{A6})$$

APPENDIX B: CALCULATION OF THE MIXING COEFFICIENT

Using the relations

$$\delta_{m,k} = \oint_{|z|<1} \frac{dz}{2\pi i} z^{k-m-1}, \quad \binom{m}{k} = \oint_{|z|<1} \frac{dz}{2\pi i} \frac{1}{z^{k+1}(1-z)^{m-k+1}}, \quad (\text{B1})$$

we can transform Eq. (20) for $\tilde{\varphi}_l(m,m';n^+,n-n^+)$ to

$$\tilde{\varphi}_l(m,m;n^+,n-n^+) = \oint \frac{dz_1}{2\pi i} \frac{1}{z_1^{m+1}} \oint \frac{dz_2}{2\pi i} \frac{1}{z_2^{m'+1}} \oint \frac{dz_3}{2\pi i} \frac{1}{z_3^{n^++1}} \oint \frac{dz_4}{2\pi i} \frac{1}{z_4^{n-n^++1}} \left\{ \frac{(1+z_1)(1+z_2)-z_3z_4}{(1-z_3)(1-z_4)-z_1z_2} \right\}^l. \quad (\text{B2})$$

Substituting $z = z_1z_2$, the dominant contribution for $m \gg 1$ comes from the pole at $z = (1-z_3)(1-z_4)$. Integrating over this new variable gives

$$\begin{aligned} \tilde{\varphi}_l(m,m';n^+,n-n^+) &= \frac{(m+l-1)!}{(l-1)!m!} \oint \frac{dz_2}{2\pi i} \frac{1}{z_2^{m'-m+l+1}} \oint \frac{dz_3}{2\pi i} \frac{1}{z_3^{n^++1}} \oint \frac{dz_4}{2\pi i} \frac{1}{z_4^{n-n^++1}} \\ &\quad \times \frac{[(z_2+(1-z_3)(1-z_4))(1+z_2)-z_2z_3z_4]^l}{(1-z_3)^{m+l}(1-z_4)^{m+l}}. \end{aligned} \quad (\text{B3})$$

The remaining integrals are done in a similar way, resulting in

$$\tilde{\varphi}_l(m,m';n^+,n-n^+) = \frac{(2l)!(m+l+n^+-1)!(m+l+n-n^+-1)!}{(m'-m+l)!(m-m'+l)!(m+l-1)!n^+!(n-n^+)!(l-1)!m!}. \quad (\text{B4})$$

Now we can collect all n^+ - and $\overline{n^+}$ -dependent terms in Eq. (21) and sum over n^+ and $\overline{n^+}$, introducing the mixing function Φ_k from Eq. (28). For large m , we can use Stirlings formula

$$\lim_{m \rightarrow \infty} \frac{(m+a)!}{(m+b)!} m^{b-a} = 1 \quad (\text{B5})$$

to obtain

$$\Phi_k(m,\bar{m},m',\bar{m}',n,\bar{n}) = \sum_{l=0}^k \frac{(1+e^{-4i\pi(\phi/\phi_0)})^{n+\bar{n}}}{(l-1)!(k-l-1)!n!\bar{n}!} \binom{k}{l} \binom{2l}{m-m'+l} \binom{2k-2l}{\bar{m}-\bar{m}'+l}. \quad (\text{B6})$$

Taking into account $Q^*(m,\bar{m},n;x) = Q^*(m,n;x) \delta_{m,\bar{m}}$, this gives Eq. (33). For $m,m' \gg 1$, the summations over l and m' can be done. Following Ref. 51, we denote $\Delta m = m - m'$, with $\Delta m \ll m$ for large m . The significant contributions to Eq. (33) come from $Q^*(m-\Delta m,n;x) \approx Q^*(m,n;x)$. Hence we can rewrite Eq. (33) as

$$\langle \rho^k(\epsilon, \phi; L) \rangle = \left(\frac{\rho_0}{2} \right)^k \sum_{m=0}^{\infty} \sum_{n=0}^{\infty} \left[\cos \left(2\pi \frac{\phi}{\phi_0} \right) \right]^{2n} e^{-[2\eta L/v(\epsilon)]n} \frac{2^{2n} m^{k+2n-2} k!}{(n!)^2} Q^{*2}(m, n; x) \sum_{l=0}^k \binom{k}{l} \sum_{\Delta m=-k}^k \binom{2l}{l+\Delta m} \times \binom{2k-2l}{k-l+\Delta m} \frac{1}{(l-1)!(k-l-1)!}. \quad (\text{B7})$$

The last two sums result in

$$\frac{2(k-1)}{k(2k-1)} \frac{\Gamma^2(2k)}{\Gamma^5(k)} \quad (\text{B8})$$

which is used in the final result for the k th moment of the DOS, Eq. (34).

*Permanent address: Azerbaijan Academy of Sciences, Institute of Physics, H. Cavid Street 33, Baku, Azerbaijan.

- ¹B. L. Altshuler, A. G. Aronov, and B. Z. Spivak, Pis'ma Zh. Éksp. Teor. Fiz. **33**, 101 (1981) [JETP Lett. **33**, 94 (1981)].
- ²D. Y. Sharvin and Y. V. Sharvin, Pis'ma Zh. Éksp. Teor. Fiz. **34**, 285 (1981) [JETP Lett. **34**, 272 (1981)].
- ³R. A. Webb, S. Washburn, C. P. Umbach, and R. B. Laibowitz, Phys. Rev. Lett. **54**, 2696 (1985).
- ⁴V. Chandrasekhar, M. J. Rooks, S. Wind, and D. E. Probe, Phys. Rev. Lett. **55**, 1610 (1985).
- ⁵S. Washburn and R. A. Webb, Adv. Phys. **35**, 375 (1986).
- ⁶A. G. Aronov and Y. V. Sharvin, Rev. Mod. Phys. **59**, 755 (1987).
- ⁷M. Büttiker, Y. Imry, and R. Landauer, Phys. Lett. **96A**, 365 (1983).
- ⁸R. Landauer and M. Büttiker, Phys. Rev. Lett. **54**, 2049 (1985).
- ⁹H.-F. Cheung, Y. Gefen, E. K. Riedel, and W.-H. Shih, Phys. Rev. B **37**, 6050 (1988).
- ¹⁰H.-F. Cheung, E. K. Riedel, and Y. Gefen, Phys. Rev. Lett. **62**, 587 (1989).
- ¹¹Y. Imry, *Introduction to Mesoscopic Physics* (Oxford University Press, New York, 1997).
- ¹²L. P. Levy, G. Dolan, J. Dunsmuir, and H. Bouchiat, Phys. Rev. Lett. **64**, 2074 (1990).
- ¹³V. Chandrasekhar, R. A. Webb, M. J. Brady, M. B. Ketchen, W. J. Gallagher, and A. Kleinsasser, Phys. Rev. Lett. **67**, 3578 (1991).
- ¹⁴D. Mailly, C. Chapelier, and A. Benoit, Phys. Rev. Lett. **70**, 2020 (1993).
- ¹⁵B. Reulet, M. Ramin, H. Bouchiat, and D. Mailly, Phys. Rev. Lett. **75**, 124 (1995).
- ¹⁶G. Montambaux, H. Bouchiat, D. Sigeti, and R. Friesner, Phys. Rev. B **42**, 7647 (1990).
- ¹⁷H. Bouchiat, G. Montambaux, and D. Sigeti, Phys. Rev. B **44**, 1682 (1991).
- ¹⁸M. Murat, Y. Gefen, and Y. Imry, Phys. Rev. B **34**, 659 (1986).
- ¹⁹M. Büttiker, Y. Imry, R. Landauer, and S. Pinhas, Phys. Rev. B **31**, 6207 (1985).
- ²⁰Y. Chen, S.-J. Xiong, and S. N. Evangelou, Phys. Rev. B **56**, 4778 (1997).
- ²¹H. Bouchiat and G. Montambaux, J. Phys. (France) **50**, 2695 (1989).
- ²²F. von Oppen and E. K. Riedel, Phys. Rev. Lett. **66**, 84 (1991);
- ²³B. L. Altshuler, Y. Gefen, and Y. Imry, Phys. Rev. Lett. **66**, 88 (1991).
- ²⁴A. Schmid, Phys. Rev. Lett. **66**, 80 (1991).
- ²⁵K. B. Efetov, Phys. Rev. Lett. **66**, 2794 (1991).
- ²⁶P. Kopietz and K. B. Efetov, Phys. Rev. B **46**, 1429 (1992).
- ²⁷P. Kopietz, Phys. Rev. B **46**, 2280 (1992).
- ²⁸J. Fricke and P. Kopietz, Phys. Rev. B **52**, 2728 (1995).
- ²⁹T. Guhr, A. Müller-Groeling, and H. A. Weidenmüller, Phys. Rep. **299**, 189 (1998).
- ³⁰V. Ambegaokar and U. Eckern, Phys. Rev. Lett. **65**, 381 (1990).
- ³¹A. Müller-Groeling, H. A. Weidenmüller, and C. H. Lewenkopf, Europhys. Lett. **22**, 193 (1993).
- ³²A. Müller-Groeling and H. A. Weidenmüller, Phys. Rev. B **49**, 4752 (1994).
- ³³M. Abraham and R. Berkovits, Phys. Rev. Lett. **70**, 1509 (1993).
- ³⁴G. Bouzerar, D. Poilblanc, and G. Montambaux, Phys. Rev. B **49**, 8258 (1994).
- ³⁵H. Kato and D. Yoshioka, Phys. Rev. B **50**, 4943 (1994).
- ³⁶T. Giamarchi and B. S. Shastry, Phys. Rev. B **51**, 10 915 (1995).
- ³⁷M. Ramin, B. Reulet, and H. Bouchiat, Phys. Rev. B **51**, 5582 (1995).
- ³⁸E. A. Jagla and C. A. Balseiro, Phys. Rev. Lett. **70**, 639 (1993).
- ³⁹H. Mori, Phys. Rev. B **51**, 12 943 (1995).
- ⁴⁰N. F. Mott and W. D. Twose, Adv. Phys. **10**, 107 (1961).
- ⁴¹V. L. Berezinskii, Zh. Éksp. Teor. Fiz. **65**, 1251 (1973) [Sov. Phys. JETP **38**, 620 (1974)].
- ⁴²A. A. Gogolin, Phys. Rep. **86**, 1 (1982).
- ⁴³B. L. Altshuler, Pis'ma Zh. Éksp. Teor. Fiz. **41**, 530 (1985) [JETP Lett. **41**, 648 (1985)].
- ⁴⁴P. A. Lee and A. D. Stone, Phys. Rev. Lett. **55**, 1622 (1985).
- ⁴⁵B. L. Altshuler, P. A. Lee, and R. A. Webb, *Mesoscopic Phenomena in Solids* (North-Holland, Amsterdam, 1991).
- ⁴⁶F. Wegner, Z. Phys. B: Condens. Matter **35**, 209 (1980).
- ⁴⁷B. L. Altshuler, V. E. Kravtsov, and I. V. Lerner, Zh. Éksp. Teor. Fiz. **91**, 2276 (1986) [Sov. Phys. JETP **64**, 1352 (1986)].
- ⁴⁸B. L. Altshuler and B. I. Shklovskii, Zh. Éksp. Teor. Fiz. **91**, 220 (1986) [Sov. Phys. JETP **64**, 127 (1986)].
- ⁴⁹V. I. Melnikov, Fiz. Tverd. Tela (Leningrad) **23**, 782 (1981) [Sov. Phys. Solid State **23**, 444 (1981)].
- ⁵⁰A. A. Abrikosov, Solid State Commun. **37**, 997 (1981).
- ⁵¹B. L. Altshuler and V. N. Prigodin, Zh. Éksp. Teor. Fiz. **95**, 348 (1989) [Sov. Phys. JETP **68**, 198 (1989)].
- ⁵²V. N. Prigodin, N. F. Hashimzade, and E. P. Nakhmedov, Z. Phys. B: Condens. Matter **81**, 209 (1990).
- ⁵³V. I. Melnikov, Fiz. Tverd. Tela (Leningrad) **22**, 2404 (1980) [Sov. Phys. Solid State **22**, 1398 (1980)].
- ⁵⁴F. J. Dyson, Phys. Rev. **92**, 1331 (1953).

- ⁵⁵M. Weissman and N. V. Cohan, *J. Phys. C* **8**, 109 (1975).
- ⁵⁶L. P. Gorkov and O. N. Dorokhov, *Solid State Commun.* **20**, 789 (1976).
- ⁵⁷J. E. Hirsch and T. P. Eggarter, *Phys. Rev. B* **14**, 2433 (1976).
- ⁵⁸A. A. Ovchinnikov and N. S. Erikhman, *Pis'ma Zh. Éksp. Teor. Fiz.* **25**, 197 (1977) [*JETP Lett.* **25**, 180 (1977)].
- ⁵⁹A. A. Ovchinnikov and N. S. Erikhman, *Zh. Éksp. Teor. Fiz.* **73**, 650 (1977) [*Sov. Phys. JETP* **46**, 340 (1977)].
- ⁶⁰A. A. Gogolin and V. I. Melnikov, *Zh. Éksp. Teor. Fiz.* **73**, 706 (1977) [*Sov. Phys. JETP* **46**, 369 (1977)].
- ⁶¹A. A. Gogolin, *Zh. Éksp. Teor. Fiz.* **77**, 1649 (1979) [*Sov. Phys. JETP* **50**, 827 (1979)].